Available online at www.sciencedirect.com
SCIENCE DIRECT®
Journal of Molecular Catalysis A: Chemical 238 (2005) 163–174
JOURNAL OF MOLECULAR CATALYSIS A: CHEMICAL
www.elsevier.com/locate/molcata

Ionic liquid structure effect upon reactivity of toluene carbonylation: 1. Organic cation structure

Ernesto J. Angueira [1], Mark G. White *

School of Chemical and Biomolecular Engineering, Georgia Institute of Technology, Atlanta, GA, USA

Received 18 March 2005; received in revised form 29 April 2005; accepted 2 May 2005
Available online 24 June 2005

Abstract

Acidic, chloroaluminate ionic liquids (IL's) formed from combining two moles of $AlCl_3$ with 1 mol of 1-R-3-methyl-imidazolium-chloride (RMIM-Cl, R = ethyl, *n*-butyl, *n*-hexyl, *n*-octyl, *n*-dodecyl, or benzyl) were examined as conversion agents for toluene carbonylation at room temperature when HCl and CO were present in the gas phase at partial pressures of 3.04 and 8.16 atm, respectively. The solubility of HCl and CO into the ionic liquids was measured at room temperature in separate experiments to determine the effect, if any, of the cation structure upon gas solubility. Molecular modeling by semi-empirical methods (AM-1; PM3, and MNDO) were used to simulate the absorption of HCl into the IL's when R was changed.

Keywords: Ionic liquid; Carbonylation; Arene; Superacid; Modeling

1. Introduction

Mixtures of $AlCl_3$ and certain organic halide salts form room temperature, ionic liquids. The organic halide salts can be substituted pyridinium halides, or disubstituted imidazolium chlorides, $(R–C_3N_2H_5–R')Cl$, and those reported often reported in the literature are 1-ethyl-3-methyl-1*H*-imidazolium-chloride (EMIM-Cl) and 1-butyl-3-methyl-1*H*-imidazolium-chloride (BMIM-Cl). Chloroaluminate ionic liquids are designated as basic, neutral, and acidic depending on the $[O^+Cl^-]/AlCl_3$ ratio where O^+ is the organic cation. It has been observed that when a strong, Brønsted acid, such as HCl, was dissolved in acidic chloroaluminate ionic liquids, a super acid was created [1]. These types of acidic, ionic liquids have been reported as conversion agents for arene carbonylation [2], alkylation of benzene with dodecene [3], Friedel–Crafts sulfonylation [4], and Friedel–Crafts alkylations and acylations [5]. Reactivity data showed that increasing HCl partial pressure above the acidic, chloroaluminate, IL increased the initial reactivity of the toluene carbonylation reaction [6,7].

It had been established that the structure of these ionic liquids may influence the transport processes [8] and the physical properties of the ionic liquid [9,10] as a result of the intimate association between the organic cation and the anion(s). It has been shown that the cation, the R-groups on the cation, and the anion can be chosen to enhance or suppress the solubility of other compounds in the ionic liquid [10]. For example, Waffenschmidt [11], showed how the solubility of octene increased in tosylate IL's prepared from tri-*n*-R-methyl ammonium cations where R was *n*-butyl, *n*-pentyl, and *n*-hexyl. The olefin was miscible in the IL prepared from the tosylate where R = *n*-octyl. They explained the increasing olefin solubility in the IL as a result of the decreasing dipole moment when R was replaced with alkyl groups of increasing chain length.

Ohlin et al. reported the solubility of CO in several ionic liquids derived from 1-R-3-methyl-1*H*-imidazolium-chloride (RMIM-Cl) at room temperature for which the R-

* Corresponding author. Tel.: +1 404 894 2822; fax: +1 404 894 2866.
E-mail addresses: gte775w@prism.gatech.edu (E.J. Angueira), mark.white@chbe.gatech.edu (M.G. White).
[1] Tel.: +1 404 894 3598; fax: +1 404 894 2866.

1381-1169/$ – see front matter © 2005 Elsevier B.V. All rights reserved.
doi:10.1016/j.molcata.2005.05.005

group was changed from methyl to octyl when the anion was either bis(trifluoromethylsulfonyl)imide or BF_4^- [12]. They showed that the CO Henry's law constant, $K_H = P_{CO}/x_{CO}$, decreased from a value of 1.34 kbar with R = methyl to a value of 0.67 kbar for R = octyl. When R was benzyl, the Henry's law constant was 1.41 kbar suggesting that the π-electron system of the benzyl group leads to decreased CO solubility in the IL. The CO solubility in these IL's was similar to that observed for CO in toluene at room temperature (K_H = 1.29 kbar) which results in very small mole fractions of CO in the toluene under a CO partial pressure of 1 atm (x_{CO} ~0.001).

For the toluene carbonylation reaction in IL's for which a gaseous Brønsted acid (HCl) was added, the solubilities of toluene, CO, and HCl were important to the reactivity in the IL. Thus, one might imagine that an optimum "design" for the IL could exist which considers the solubility of gaseous species, such as CO and HCl, as well as the solubility of liquid species, such as toluene, in the ionic liquid. Apart from reactant solubility, one must also consider other factors that influence the formation of reactive species in the IL, such as strongly acidic species.

Carey and Sundberg [13] reported in their book that the strength of association between species depended upon LUMO and HOMO energies and the symmetries of the orbitals. Researchers studied the effect of changing structure and its effect on the MOs using the approach of the perturbation molecular orbital theory [14], and the interactions of orbitals in reacting molecules by incorporating the concept of frontier orbital control, which proposes that the most important interactions will be between a particular pair of orbitals [15]. These considerations have led investigators to examine the molecular environment of ionic liquids so as to understand better the experimental characterizations of these systems. Dieter et al. showed that the imidazolium cations and the chloroaluminate anions with the chlorides are closely associated to form layers in the neutral and basic IL's. [16] Moreover, Chandler and Johnson, showed how the formation of certain reactive chloroaluminate species, such as the Brønsted super acid ($HAl_2Cl_8^-$) and the Lewis super acid ($Al_2Cl_7^-$) depended upon the free energy of formation of the species in the melt [17] and Angueira [18] showed how the partial pressure of HCl above the melt determined the relative mole fractions of the Brønsted to Lewis super acid species. Several structures (monomeric [1] and dimeric [17,18] Al species) have been proposed for the Brønsted super acid species; therefore, it is appropriate to model these and other structures that might be present in the IL to determine how the solubility of HCl may be influenced by the structure of cation present in the IL.

We hypothesize that the structure of IL can (1) control the solubility of the gaseous reactants, (2) promote the formation of reactive species, and (3) therefore influence the reactivity of system towards a substrate. This hypothesis will be tested by experimental and by molecular modeling efforts in which the IL's would be formed from $AlCl_3$ (2 mol) and members of a family of 1-R-3-methyl-imidazolium-chloride (RMIM-Cl, 1 mol), where R = ethyl, *n*-butyl, *n*-hexyl, *n*-octyl, *n*-dodecyl, or benzyl. The modeling of HCl solubility in these IL's will describe the free energy for the formation of HCl-adducts with the IL's when R is changed. Where appropriate, the molecular modeling may indicate when more than one HCl-adduct can be formed. These model predictions will be compared to experimentally determined, room temperature, absorption equilibrium constants for HCl in the ionic liquids as a function of R for gas pressures up to 3.04 atm. Finally, we will determine by experiment the effect of R upon the reactivity of a toluene carbonylation probe reaction completed at room temperature in the presence of HCl (3.04 atm) with CO added to a total pressure of 11.2 atm.

2. Experimental

2.1. Chemicals

The imidazolium compounds 1-ethyl-3-methyl-imidazolium-chloride (EMIM-Cl), 1-butyl-3-methyl-imidazolium-chloride (BMIM-Cl), and 1-hexyl-3-methyl-imidazolium-chloride (HMIM-Cl), were obtained from Sigma–Aldrich; whereas, 1-octyl-3-methyl-imidazolium-chloride (OMIM-Cl), 1-dodecyl-3-methyl-imidazolium-chloride (DoMIM-Cl), and 1-benzyl-3-methyl-imidazolium-chloride (BeMIM-Cl), were obtained from Merck Chemicals and used without further purification. Aluminum chloride (99.99%), obtained from Sigma–Aldrich, was sublimed under vacuum before use. Toluene (anhydrous, 99.8%) was obtained from Sigma–Aldrich and used without further purification. Carbon monoxide, CP grade, and HCl (anhydrous, 99+%) were obtained from Airgas and Sigma–Aldrich, respectively.

2.2. Preparation of IL's

The weighing instrument, chemicals, were placed in a AtmosBag filled with dry Ar. $AlCl_3$ was weighed, and $RMIM^+$-Cl^- was added so as to obtain the desired $AlCl_3$/$RMIM^+$-Cl^- molar ratio. Details of the preparation can be found elsewhere [7].

2.3. Absorption of HCl gas in IL's

The amounts of HCl gas absorbed by the IL's were determined using a volumetric apparatus from a measurement of the system volumes, gas pressures, and temperatures. The moles absorbed were computed using the ideal gas law. A calibrated stainless steel vessel (150 cm^3) was filled initially with HCl at room temperature and the pressure was measured to the nearest 0.1 psia (0.0068 atm) using a 750B Baratron Pressure Transducers with a type LDM-B display module. This level of uncertainty in measuring the gas pressure leads to a minimum detection limit of 0.003 in the mole fraction of the absorbate in the IL. The gas in this vessel was expanded into the Fisher–Porter reaction tube that contained a known

amount of the IL at room temperature. All IL's were stirred at 1000 rpm during the absorption experiment except for the one IL derived from 1-dodecyl-3-methyl-imidazolium-chloride, which could only be stirred at 300 rpm, and the one derived from 1-benzyl-3-methyl-imidazolium-chloride which could only be stirred at 475 rpm due to their high viscosity. From these data, the amount of gas remaining in the gas phase could be calculated before and after the expansion. The system was evacuated and the absorption repeated to determine if the process was reversible. That is, the amount of HCl absorbed was the same in subsequent runs for which the system was evacuated at room temperature between absorption runs. Care was taken to remove the gas dissolved in the IL sample initially, but this is easily accomplished because no volatization of the IL occurs during the evacuation process. The dead volume of the apparatus was determined using Ar for each partial pressure of gas studied at room temperature. The partial pressures of HCl were varied from 0 to 3.04 atm.

A control was completed for the absorption of HCl gas into toluene at room temperature for HCl partial pressures between 0 and 3.04 atm. Subsequently, the HCl absorption was determined at room temperature above the neat, acidic IL's derived from $AlCl_3$ and RMIM-Cl in the ratio of 2/1 mol (R = ethyl, *n*-butyl, *n*-hexyl, *n*-octyl, *n*-dodecyl, and benzyl). One more test was completed for the acidic IL developed from $AlCl_3$/BMIM-Cl (2/1 mol) and toluene (1 mol toluene/mol $AlCl_3$) over the range of HCl partial pressures of 0 to 3.04 atm.

2.4. Absorption of CO gas in IL's

The amounts of CO gas absorbed by the IL's [$AlCl_3$/RMIM-Cl = 2/1 mol; R = ethyl, *n*-butyl, *n*-hexyl, *n*-octyl, *n*-dodecyl, and benzyl] were determined using the same volumetric apparatus and procedure as described in the absorption of HCl section. The partial pressures of CO were varied from 0 to 6.80 atm. The minimum detection limit for CO mole fraction in the IL's was 0.003 in the mole fraction (vide supra).

2.5. Absorption of HCl + Ar and HCl + CO mixtures in IL's

Experiments using acidic IL and gas mixtures of either HCl + Ar or HCl + CO were conducted to determine if HCl enhanced the CO solubility in the IL. The lower detection limit for CO may prevent us from actually observing any enhanced CO solubility. In the volumetric apparatus 2.02 atm HCl and Ar were mixed for a total pressure of 7.22 atm. The gas mixture was expanded into the acidic IL. The same procedure was repeated for HCl and CO mixture. It was expected here, that Ar would be a non-absorbing gas.

2.6. Reaction studies—Low pressure

Low pressure reactions were completed in a Fisher–Porter glass tube affixed with a stirring magnet that was placed in an AtmosBag. The desired chloroaluminate/$RMIM^+$-Cl^- IL was weighed into the Fisher–Porter tube (∼8 g) and dry toluene (3.5 cm^3) was added to obtain the desired Al^{3+}/toluene ratio: 1/1 mol. The reactor was sealed, removed from the AtmosBag and purged with HCl gas before HCl gas was added to the desired partial pressure and then this mixture was stirred for 1/2 h at room temperature. Carbon monoxide was then added to give a total pressure of 11.2 atm. The reaction temperature was room temperature and the CO pressure was monitored at the beginning of the experiment to verify CO consumption. After the reaction was completed, the reactor was slowly vented and purged with Ar. The mixture was poured into a separatory funnel filled with an ice/distilled water mixture so as to dilute the acidic components. The organic layer was collected after it was neutralized with a saturated sodium bicarbonate solution. Previous experiments [19] with trifluoromethane sulfonic acid (HOTf) showed that a stirring rate of 800 rpm was sufficient to overcome mass transfer resistance. Since the conversion rate in the IL [7] is similar to that for HOTF (vide infra) when the acid/substrate = 10 mol/mol, we will use a similar stirring rate of 1000 rpm.

A control experiment was completed for which no IL was added to the reaction mixture described above but the reaction was continued for 18 h. The product mixture when worked up and analyzed by GC/MS showed no aldehyde, which confirmed the inactivity of the system without the IL.

2.7. Analytical

Organic products were analyzed in a HP-5890 Series II Plus GC equipped with a HP-5972 mass spectrometer. High purity helium (99.995%, Airgas) was the carrier gas and the column was 15 m long, 0.25 mm i.d., and 0.25 μm film thickness obtained from Supelco (SPB-5 24032). An analytical method was developed to separate all the liquid phase products using the following GC oven protocol: initial temperature is 35 °C, hold for 5 min, then increase temperature 10 °C per minute, and finally hold temperature at 180 °C for the final 5.50 min.

2.8. Modeling of the IL's for HCl solubility

Semi-empirical methods (AM-1, PM3 and MNDO) were used to (1) optimize the geometry of species in the IL's such as 1-R-3-Me-imidazolium cation, $AlCl_4^-$, $Al_2Cl_7^-$, and $HAl_2Cl_8^-$, and (2) calculate the thermodynamic properties of these equilibrium structures. Although some earlier investigators speculated on the formation of monomeric, Al Brønsted acidic species ($HAlCl_4$), Zawodzinski showed that molecular HCl could be detected in acidic $AlCl_3$–EMIM-Cl [20], and our previous modeling showed that $HAlCl_4$ and $HAlCl_4^-$ were not present in these IL's when the HCl pressure was less than 30 atm [18]. These results may be placed in the context of the older literature where

Brown showed that HCl does not react with $AlCl_3$ to form $HAlCl_4$ [21] and thus suggested that this substance only exists as ion pairs at the conditions of their measurements.

3. Results

3.1. Modeling of IL's

Preliminary modeling began by constructing the IL with the following species: $AlCl_3$, $AlCl_4^-$, HCl, and $EMIM^+$. The optimized geometry (PM3) depended upon the initial starting positions of these species which was determined by a MM2 preliminary geometry optimization (Fig. 1).

In every case, the $AlCl_3$ and $AlCl_4^-$ associated to form a pair with a short distance between the coordinately unsaturated site of the $AlCl_3$ and a Cl from either the $AlCl_4^-$ or the Cl of the bridging HCl. The HCl was located in three distinctive structures: (1) between the $AlCl_3$ and $AlCl_4$ anion to form Fig. 1a ($\Delta G_f^\circ = -428.7$ kcal/mol); (2) between the anion and cation (Fig. 1b; $\Delta G_f^\circ = -427.7$ kcal/mol), or (3) associated with the cation (Fig. 1c; $\Delta G_f^\circ = -425.1$ kcal/mol). Since the aluminum species always appeared as a pair, and since earlier modeling work by Chandler and Johnson [17] supports a dimeric Al species as the structured favored in acidic, chloroaluminates, subsequent modeling efforts will examine the dimeric anion $Al_2Cl_7^-$ as the building block for the anionic species in these acidic IL's and these results will be compared to the free energies of the optimized geometries for these structures with the free energies of formation that were developed from monomeric chloroaluminate species so as to determine the structure(s) of the thermodynamically favored, chloroaluminate species in equilibrium with HCl.

The modeling of the IL by semi-empirical methods revealed three possible optimized structures, Fig. 2, that developed upon absorption of HCl gas at room temperature. As an example, consider the results from the PM3 model which shows the HCl inserted into the $Al_2Cl_7^-$ anion to form a bridging species (Fig. 2a). In the second structure, HCl was associated with the $Al_2Cl_7^-$ anion through a terminal Cl and also associated with the imidazolium cation through the C-2 proton (Fig. 2b). The third structure shows the HCl species involved with the cation only (Fig. 2c). The free energies of formation for each of these three species at 298 K were as follows: Fig. 2a, −428.93 kcal/mol; Fig. 2b, −430.59 kcal/mol; and Fig. 2c, −427.26 kcal/mol. These free energies of formation were lower for the chloroaluminate species appearing as the anionic dimer ($Al_2Cl_7^-$) rather than as the pair of species ($AlCl_3$/$AlCl_4^-$). The dimer structures were favored by 0.23 kcal/mol (Fig. 2a versus Fig. 1a), 2.9 kcal/mol (Fig. 2b versus Fig. 1b), and 2.2 kcal/mol (Fig. 2c versus Fig. 1c). Considering the accuracy of the predictions (±4.0–5.0 kcal/mol) [22] the dimers (Fig. 2) would appear to show a free energy of formation similar to the corresponding structures in Fig. 1. For HCl placed between the anion and cation, changes in either the cation or the anion would affect the amount of HCl absorption into the IL and thus could have a direct influence of the reactivity of the IL for Brønsted-demanding reactions. On the other hand, HCl attached to structure in Fig. 2a would be largely influenced by the type of anion metal chloride; whereas, HCl absorption in structure in Fig. 2c would influenced mainly by changes in the structure of the imidazolium cation. One can interrogate the degree of influence these structural changes in the cation might have on the HCl absorption equilibria by calculating the free energy change associated with the following

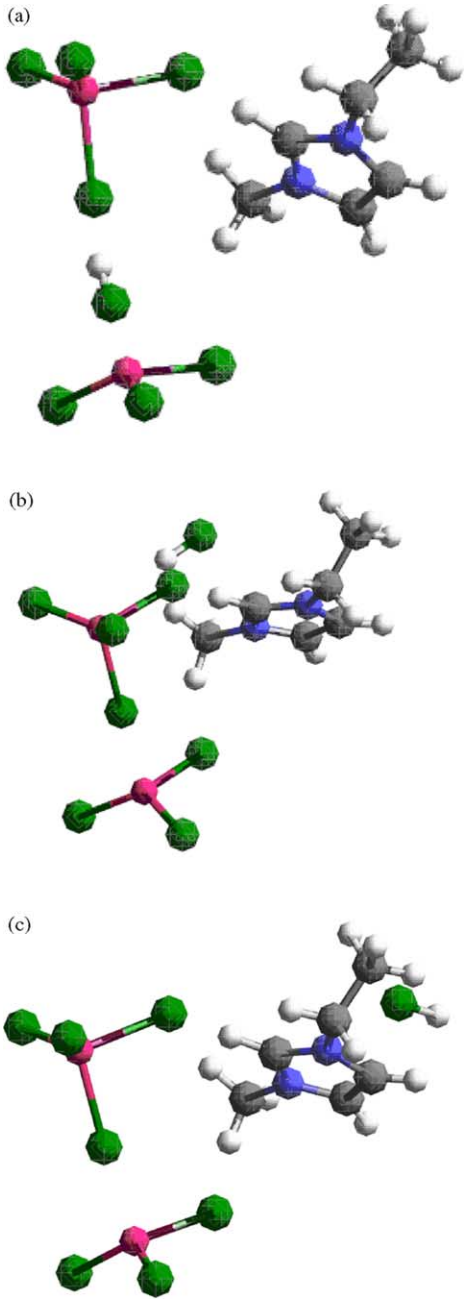

Fig. 1. (a) −428.7 kcal/mol; (b) −427.7 kcal/mol; (c) −425.12 kcal/mol.

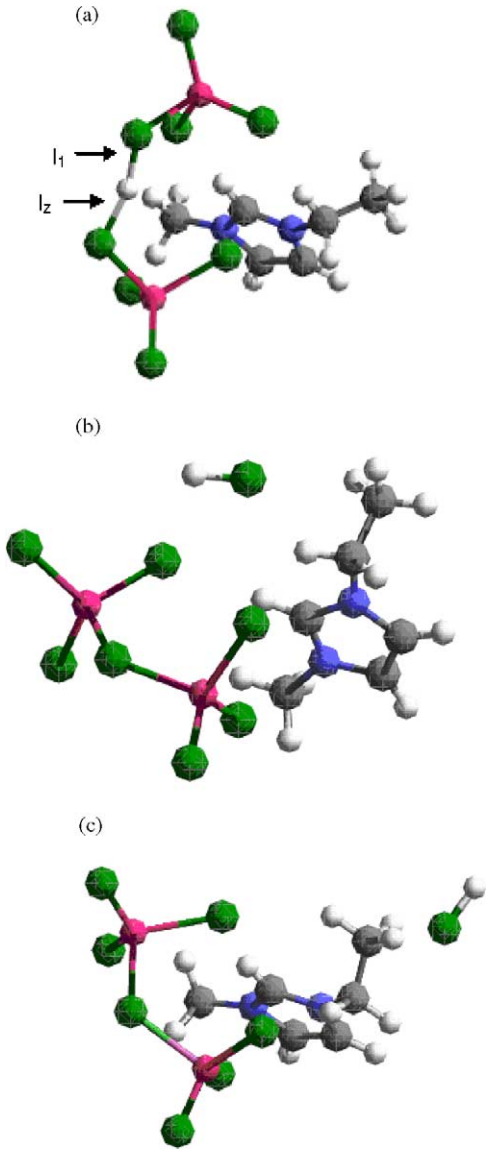

Fig. 2. Three structures for siting of HCl in $EMIM^+$–$Al_2Cl_7^-$ ionic liquid: (a) ClHCl bridging ($AlCl_3$) polyhedra; (b) HCl between anion and cation; (c) HCl near cation.

equation to model HCl absorption:

$$\{RMIM^+\,Al_2Cl_7^-\} + HCl \Leftrightarrow \{RMIM^+\,HCl\,Al_2Cl_7^-\} \quad (1)$$

We show here the free energies of formation for the three structures of the absorbed species as R was changed using three semi-empirical quantum mechanical programs: AM-1, PM3, and MNDO (Tables 1–3).

Two of three models (AM-1 and MNDO) predicted the highest values of the free energies of absorption for HCl absorption at Fig. 2a site. The PM3 predictions show that no one site for the HCl is favored for each and every cation. If one considers the inaccuracy in these predictions for the free energy (±4.0–5.0 kcal/mol) [22], siting of HCl at Fig. 2b and c sites show about the same free energy of absorption from the predictions of the MNDO model. The AM-1 model shows similar $\Delta G_{absorption}$ for structures in Fig. 2b and c for all R. The PM3 predictions show the same $\Delta G_{absorption}$ for Fig. 2b and c sites only for the cations ethyl, butyl, benzyl, and octyl.

The H–Cl bond length can be estimated using the semi-empirical models and all three models (AM-1, PM3, and MNDO), show that the HCl bond length depends upon the structure in Fig. 2a–c but a systematic change in the bond length was not observed for changing R. All three models showed that structure in Fig. 2a exhibit similar HCl bond length (1.52–1.60 Å), and this bond is I_1 in Fig. 2a. For most cases of R, AM1 and MNDO predicted that bond I_2 was longer than I_1 (1.59–1.63 Å) while PM3 predcited I_2 to be the similar to I_1 (1.51–1.53). The three models demonstrated that the H–Cl bond length for Fig. 2c structure was the shortest, often very similar to the bond length predicted for the isolated gas phase molecule by the same model (1.284 Å for AM1, 1.268 Å for PM3, and 1.348 Å for MNDO). Predicted values for the H–Cl bond lengths in structure in Fig. 2b were 1.32 Å for AM1, 1.34–1.35 Å for PM3, and 1.35 Å for MNDO. From these predictions, one might infer that the H–Cl bond length may depend upon its environment, being longest when associated with the chloroaluminate anion, shortest when associated with the cation, and of some intermediate bond length when associated with both anion and cation as in the structure Fig. 2b. HCl bond length may be significant as it relates to the reactivity of the H–Cl species for protonation and reaction in the toluene carbonylation reaction. In a control experiment where no IL was present, no conversion of toluene was observed after 18 h of reaction in HCl and CO at the conditions that produced significant conversion to *p*-tolualdehyde when the IL was present.

When this system without the IL was modeled with AM-1, PM3, or MNDO the HCl would associate with the toluene (Fig. 3) and the H–Cl bond length was no longer than that predicted for the gaseous, isolated HCl molecule by each model. This result shows that the bond length of the H–Cl molecule predicted from the semi-empirical methods may be used in conjunction with the reactivity of the reference system to estimate the relative reactivity of the unknown systems containing the IL. That is, we suggest that HCl sited in Fig. 2c structures are likely to be unreactive towards catalyzing the toluene carbonylation reaction from a consideration of the predicted H–Cl bond lengths being similar to the HCl bond length in the isolated molecule; whereas the HCl sited in Fig. 2a and b structures could be reactive towards toluene carbonylation owing to the longer H–Cl bond lengths predicted for these structures. These predictions suggest that at least three absorption sites could be developed when HCl contacts the IL's described here and that the reactivity of the HCl may depend upon its location in the IL structure.

3.1.1. Predictions—effect of changing R

Now consider the trends in the predicted results for changing R for HCl absorbed between the cation and anion (structure Fig. 2b) and how this change affects the free energy of HCl absorption as predicted from the AM-1, PM3, and

Table 1
$\Delta G_{absorption}$ for HCl into $RMIM^+$–$Al_2Cl_7^-$ IL and HCl bond length (AM-1)

Alkyl group, R	$\Delta G_{absorption}$, kcal/mol			HCl bond length, Å (gas phase = 1.28 Å)			
	Fig. 2a	Fig. 2b	Fig. 2c	Fig. 2a (I_1)	Fig. 2a (I_2)	Fig. 2b	Fig. 2c
Ethyl	11.7	3.4	2.8	1.53	1.63	1.32	1.29
Butyl	11.9	5.5	4.6	1.55	1.61	1.32	1.29
Benzyl	11.4	4.2	6.2	1.53	1.63	1.32	1.29
Hexyl	13.8	3.3	7.1	1.56	1.61	1.32	1.29
Octyl	12.6	3.6	7.4	1.53	1.63	1.32	1.29
Dodecyl	18.4	4.0	8.3	1.53	1.64	1.32	1.29

Table 2
$\Delta G_{absorption}$ for HCl into $RMIM^+$–$Al_2Cl_7^-$ IL and HCl bond length (PM3)

Alkyl group, R	$\Delta G_{absorption}$, kcal/mol			HCl bond length, Å (gas phase = 1.27 Å)			
	Fig. 2a	Fig. 2b	Fig. 2c	Fig. 2a (I_1)	Fig. 2a (I_2)	Fig. 2b	Fig. 2c
Ethyl	2.3	0.7	4.0	1.53	1.52	1.35	1.27
Butyl	−0.8	1.1	2.7	1.53	1.51	1.35	1.27
Benzyl	4.7	1.7	4.6	1.53	1.51	1.35	1.27
Hexyl	2.8	0.9	6.8	1.52	1.52	1.34	1.28
Octyl	−0.4	0.3	1.2	1.53	1.50	1.34	1.28
Dodecyl	4.9	0.5	6.6	1.53	1.52	1.34	1.28

Table 3
$\Delta G_{absorption}$ for HCl into $RMIM^+$-$Al_2Cl_7^-$ IL and HCl bond length (MNDO)

Alkyl group, R′	$\Delta G_{absorption}$, kcal/mol			HCl bond length, Å (gas phase = 1.35 Å)			
	Fig. 2a	Fig. 2b	Fig. 2c	Fig. 2a (I_1)	Fig. 2a (I_2)	Fig. 2b	Fig. 2c
Ethyl	15.4	3.0	3.0	1.6	1.62	1.35	1.35
Butyl	16.6	4.0	3.8	1.6	1.61	1.35	1.35
Benzyl	15.3	2.4	1.4	1.6	1.60	1.352	1.35
Hexyl	17.1	2.1	2.5	1.6	1.63	1.36	1.35
Octyl	18.9	2.8	2.2	1.6	1.62	1.35	1.35
Dodecyl	18.2	1.2	2.3	1.6	1.61	1.35	1.35

MNDO models (Tables 1–3). The free energy of HCl absorption is the same for all R-groups if one considers the error of these calculations to be ±4.0–5.0 kcal/mol regardless of the model used [22]. These free energies of absorption can be used to predict the trends in absorption amounts by recalling the relationship between the free energy of absorption and the equilibrium absorption constant, K:

$$\ln K = -\Delta G_{absorption}/RT \quad (2)$$

From a consideration of the free energies of absorption, (Table 4), it is clear that very little HCl will be absorbed as structure in Fig. 2a when using the results of the AM-1, MNDO models. The PM3 predictions suggest that all structures are equally likely.

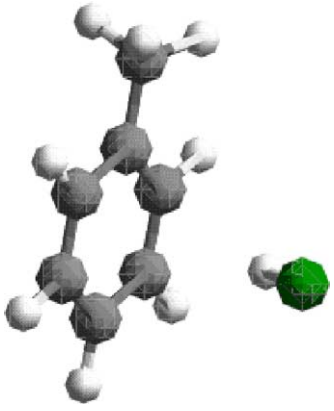

Fig. 3. Model of HCl in toluene.

3.2. HCl absorption

The HCl absorption in $AlCl_3$/$RMIM^+$-Cl^- intrinsically acidic IL's was studied at different partial pressures of HCl. The amounts of HCl absorbed as a function of time was

Table 4
Summary of predictions for all R-groups

Model	$\Delta G_{absorption}$, kcal/mol		
	Fig. 2a	Fig. 2b	Fig. 2c
AM-1	13.3	4.0	6.1
PM3	2.3	0.9	4.3
MNDO	16.9	2.6	2.5

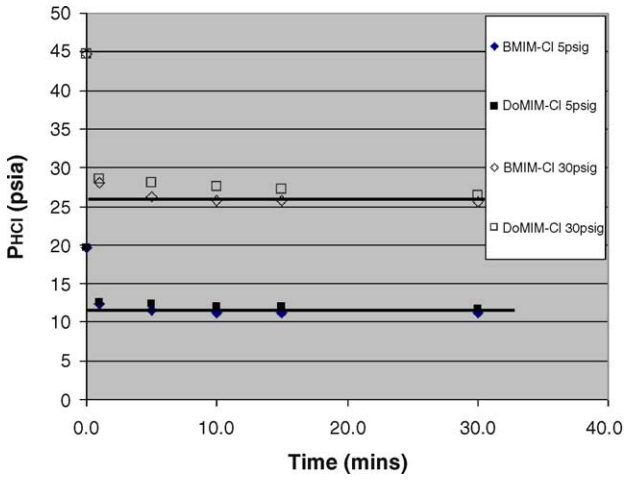

Fig. 4. Rate of HCl absorption in intrinsically acidic ionic liquids.

recorded for all RMIM-Cl IL's first at two different partial pressures (1.34 and 3.04 atm) to determine the minimum time required to confirm that equilibrium had been established. In Fig. 4 we show the data for the BMIM-Cl and DoMIM-Cl as these represent the two extremes in viscosity with the IL-derived DoMIM-Cl showing the highest viscosity. Most of the HCl was absorbed within the first 10–15 min; however, the HCl absorption rate into the DoMIM-Cl IL was consistently less than that observed into the BMIM-Cl at each sampling time. The stirring rate for the *n*-dodecyl tests was 300 rpm, for the benzyl tests it was 475 rpm, and it was 1000 rpm for all other IL's. But, the total amount HCl absorbed at 1/2 h was nearly the same for both systems thus validating the protocol used here to pretreat the IL with HCl for 1/2 h before starting the toluene carbonylation reaction.

We hypothesized that the HCl solubility in the IL's might be influenced by the size of the alkyl group in the organic cation. Fig. 5 shows the data of HCl absorption at room temperature that were developed from IL's containing RMIM–$Al_2Cl_7^-$ for R = ethyl, *n*-butyl, *n*-hexyl, *n*-octyl, *n*-dodecyl, and benzyl. We also show the error bars for three series of measurements: the *n*-butyl cation, *n*-dodecyl cation,

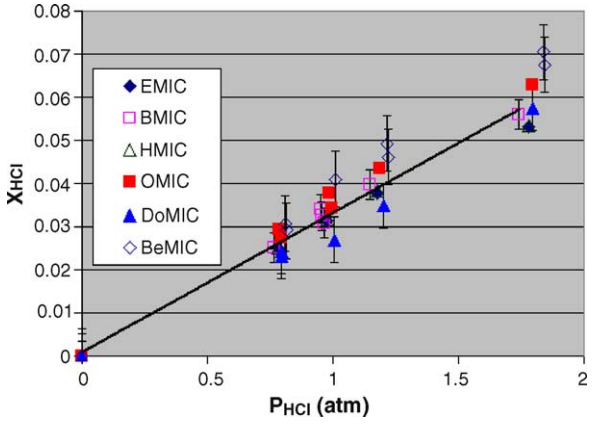

Fig. 5. HCl absorption as a function of HCl partial pressures at 298 K.

Table 5
Summary of HCl absorption data

Cations	K_i, atm^{-1}	ΔG, kcal/mol
EMIM-Cl	0.0296	2.08
BMIM-Cl	0.0323	2.03
BeMIM-Cl	0.0389	1.92
HMIM-Cl	0.0297	2.08
OMIM-Cl	0.0353	1.99
DoMIM-Cl	0.0312	2.05
All data	0.0327 ± 0.002	2.03 ± 0.04

and the benzyl cation. Most of the data were observed to be described by a single line when one considers the magnitude of the measuring errors indicated here by the error bars in Fig. 5, which represents an uncertainty of ±0.1 psia (0.0068 atm) in measuring the pressures.

For each data set from an IL, values were determined for the experimental equilibrium absorption constant and the free energy of absorption were calculated (Table 5). The average value of *K* for all of the data was 0.0327 ± 0.002 atm^{-1} and the corresponding free energy of absorption was 2.03 ± 0.04 kcal/mol.

The solubility of HCl was also studied in basic and neutral chloroaluminates IL's containing the *n*-butyl-methyl-imidazolium cation (Fig. 6). It was shown that the HCl absorption was linear with respect to the HCl pressure for the neutral and acidic IL's, but not for the basic IL. Moreover, the amount of HCl absorption was most for the intrinsically basic IL ($K_{HCl} = 0.7$ atm^{-1} when $n = 1/2$), least for the intrinsically acidic IL ($K_{HCl} = 0.0321$ atm^{-1} when $n = 2$) and the HCl absorption was intermediate to these two for the neutral IL ($K_{HCl} = 0.061$ atm^{-1} when $n = 1$) where *n* is the $AlCl_3$/RMIM$^+$-Cl$^-$ ratio. The equilibrium constant for HCl uptake in a neutral $AlCl_3$/EMIM-Cl was 0.053 atm^{-1} also measured at room temperature (Table 6). Neutral EMIM-Cl

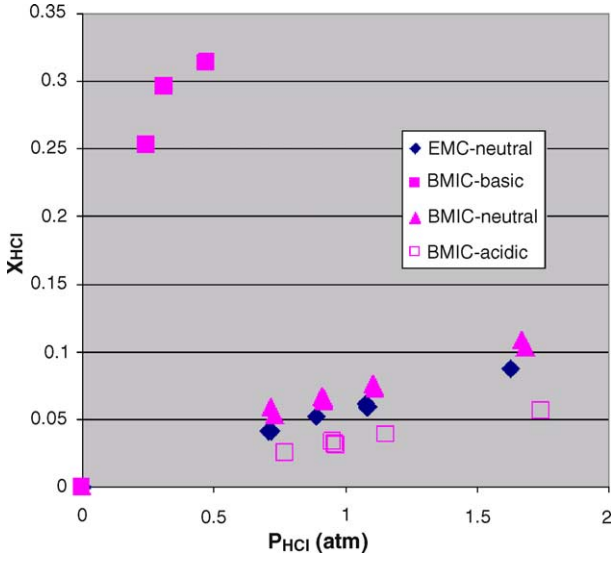

Fig. 6. HCl absorption in *n*-butyl-methyl-imidazolium *n*-$AlCl_3$.

Table 6
Summary of HCl absorption into R-methylimidazolium Cl *n*-$AlCl_3$

IL's	K_i, atm^{-1}	ΔG, kcal/mol
EMIM-Cl (neutral)	0.0531	1.738
BMIM-Cl (basic)	0.7012	0.210
BMIM-Cl (neutral)	0.0610	1.656
BMIM-Cl (acidic)	0.0323	2.033

and BMIM-Cl ionic liquids showed very similar free energies of absorption for HCl (1.6–1.7 kcal/mol). This trend that was observed for the BMIM-Cl chloroaluminates was similar to that described by Campbell and Johnson for the ionic liquid derived from the EMIM-Cl chloroaluminate they studied [23].

Additional HCl absorption studies were completed in dry toluene as a control for these studies. Toluene picked up 0.0479 mol HCl/mol toluene at room temperature and at an equilibrium pressure of 16.3 psia (1.11 atm). These data suggest an equilibrium absorption coefficient at room temperature of 0.0457 atm^{-1}. An IL derived from $AlCl_3$/BMIM-Cl (2 mol/mol) and mixed with an amount of toluene equal to the moles of $AlCl_3$ showed an HCl absorption of 0.1011 mol HCl/mol toluene in the mixture at room temperature. The equilibrium absorption coefficient for this liquid was 0.0408 atm^{-1}. The difference in the HCl absorption between these two liquids was 0.1011–0.0479 = 0.0532 mol HCl/mol toluene. This absorption amount will be compared to that of the neat IL (i.e., no toluene added) at the same conditions which shows 0.0571 mol HCl/mol $AlCl_3$ and since the moles of $AlCl_3$ equals the moles of substrate, it appears that the incremental absorption of HCl in the IL with toluene added to the IL equals that absorption in the toluene alone at the same conditions.

3.3. CO absorption

The CO absorption was studied for the different IL's described above at partial pressure of CO between 0 and 6.8 atm. While Anthony et al. were not able to detect CO solubility [24] in the IL's they studied, Ohlin et al. reported the solubility of CO increased with increasing size of the R-group chain from methyl, ethyl, *n*-butyl, *n*-hexyl, and *n*-octyl in two ionic liquids derived from RMIM-Cl with either the bis(trifluoromethylsulfonyl)imide or the tetrafluoroborate anions [12]. Using the same volumetric apparatus and procedure as in the HCl absorption, we were not able to detect any CO absorption. It may be speculated that the detection limit of our apparatus (x_{CO} ~0.003) was greater than the amount of CO that could be absorbed into these IL's. We find support for this speculation in the data reported by Ohlin et al. who showed that the CO mole fraction was ~0.001 at CO partial pressures near 1 bar for non-acidic IL's derived from the combination of the same cations but having either bis(trifluoromethylsulfonyl)imide or tetrafluoroborate anions [12].

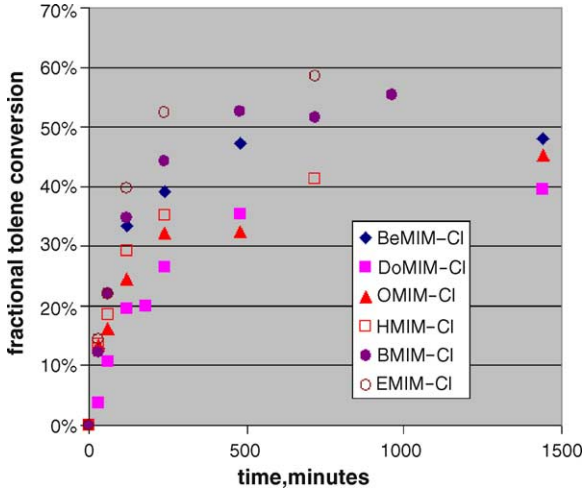

Fig. 7. Fractional toluene conversions versus time for Me-imidazolium-R cations.

3.4. Mixed gas absorption

In the gas mixtures experiments we did not observe an increase in the total moles absorbed by the HCl + CO mixture when compared to the HCl + Ar mixture.

3.5. Reactivity of IL's having different R-groups

The reactivity of the toluene carbonylation reaction at room temperature (HCl partial pressure = 3.04 atm, CO partial pressure = 8.16 atm) was determined for a series of intrinsically acidic IL's ($AlCl_3$/RMIM-Cl^+ = 2) for which the R-group was varied: ethyl, *n*-butyl, *n*-hexyl, *n*-octyl, *n*-dodecyl, and benzyl (Fig. 7).

The reactivity's of the IL's prepared from $RMIM^+$ cation having either ethyl or *n*-butyl were very similar but the cation having the *n*-butyl group appeared to be slightly lower in reactivity than the cation showing the ethyl group. However, the reactivity was systematically lower for the IL's prepared from the cations having the benzyl, *n*-hexyl, *n*-octyl, and *n*-dodecyl groups on the imidazolium ring, especially evident in the data for conversions greater than 10%. These data for reaction times less than 2 h could also be correlated by the integrated rate equation that we described earlier [6,7] as shown in Fig. 8. Data obtained at short reaction times were chosen for correlation so as to minimize the effect of the product aldehyde for inhibiting the reaction rate as was observed in reaction catalyzed by triflic acid [19]. The slope of this integrated plot is the product of the rate constant, the dissolved CO concentration, and the Brønsted acid concentration in the IL: $k[CO][H^+]$. These slopes vary as shown below:

$$\text{Ethyl} > n\text{-Butyl} > \text{Benzyl} > n\text{-Hexyl} > n\text{-Octyl} > n\text{-Dodecyl} = 4.68 > 3.92 > 3.65 > 2.98 > 2.34 > 1.35\,\text{k}\,\text{min}^{-1}$$

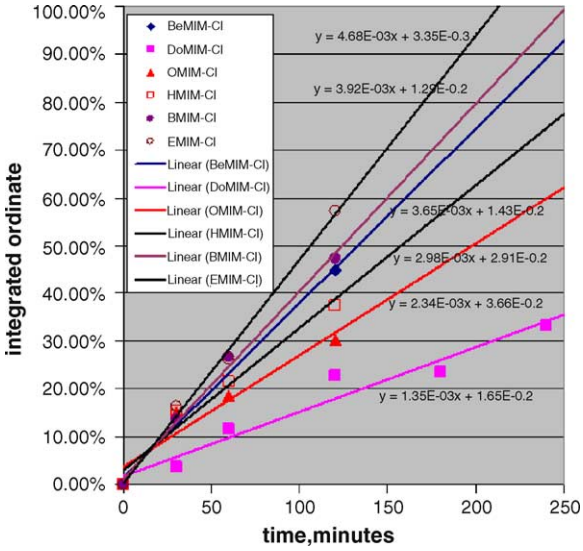

Fig. 8. Integrated rate plot: effect for changing the size of the alkyl group.

4. Discussion

Several reports [16,25] have appeared in the open literature in which the authors described their attempts to model the molecular properties of chloroaluminate ionic liquids described here. They used MNDO and AM-1 to simulate the IR vibrational spectra of O^+Cl^- and $O^+AlCl_4^-$. For the basic and neutral melts, they showed monomeric aluminum chloride species ($AlCl_4^-$) assembling around the organic cation ($EMIM^+$) to form a "sandwich compound". When excess chloride was present (as in the basic melts), it was found between the organic cations. The modeling of the present work focused on acidic melts for which excess $AlCl_3$ is present, and we revisit the question of aluminum speciation to determine if monomeric or dimeric aluminum chlorides are favored by the thermodynamics.

The modeling of the acidic chloroaluminates starting with monomeric aluminum chloride and chloroaluminate anion with HCl and the $EMIM^+$ cation shows that the aluminum species assemble into a group (Fig. 1) where the HCl is shared between the two aluminum species (structure in Fig. 1a), between the anion and the cation (structure in Fig. 1b), or on the cation (structure in Fig. 1c). The same result was observed when using any of the semi-empirical programs (AM-1, PM3, and MNDO). It is clear from this modeling that monomeric aluminum species forming a sandwich structure was not favored in the acidic melts as was observed in the neutral and basic melts. Moreover, it was clear that the monomeric aluminum species assembled into a pair in this acidic melt with HCl present. When the dimeric aluminum species ($Al_2Cl_7^-$) were employed to model the acidic melt along with HCl and the $EMIM^+$ cation, the free energies of formation for the structures that were formed (Fig. 2) were similar to the corresponding structures observed in Fig. 1. In addition, the HCl molecules sited at positions to form structures with the dimeric aluminum species that were similar to those observed in Fig. 1. Structure in Fig. 2a showed the HCl forming a compound with the $AlCl_3$ and $AlCl_4^-$ for which the H was sited between two $AlCl_4^{1-}$ species; however, the H–Cl bond distances were different when predicted by AM-1 and MNDO: 1.52 and 1.64 Å. The shorter H–Cl bond was found in that part of the structure arising from the anionic chloroaluminate that was closest to the C-2 proton of the cation. The PM3 model showed a nearly symmetrical Al_2Cl_8H anion. For structure Fig. 2b, the HCl was sited between the anion and the cation with an average H–Cl bond distance of 1.34 Å. Structure Fig. 2c showed that the HCl was sited on the cation with a bond distance similar to that predicted for an isolated HCl. Apparently, the environment for the HCl plays a role in determining the bond length, and it may play a role in determining the reactivity of these species towards the toluene carbonylation reaction. These structures showed different free energies of formation with Fig. 2c structure showing the highest free energy of formation (−427.26 kcal/mol); whereas, Fig. 2a and b structures showed lower free energies of formation (−428.9 and −430.6 kcal/mol, respectively). Similar structures were observed, when this modeling was repeated for the IL's derived from the other cations ($RMIM^+$, R = *n*-butyl, benzyl, *n*-hexyl, *n*-octyl, *n*-dodecyl). The free energy predicted by a particular model for absorption for HCl into the structures Fig. 2a–c, while different from one structure to another, did not change much for a particular structure as the R-group was changed using a particular model. Thus, it would appear that the affinity of HCl into these IL's is not influenced much by the type of R-group. In addition, the free energy for absorption predicted by AM-1 and MNDO was highest for siting the HCl on the anion between the two $AlCl_4^{1-}$ species, and it was lower for siting the HCl between the anion/cation and on the cation for IL's derived from all R-groups.

The data for HCl absorption into the IL's were collected after a sufficient time to allow for the effects of mass transfer to be absent from the data set, even for the IL's derived from *n*-dodecyl and benzyl. The data in Table 5 for K_{HCl}, show no systematic change in the values as the chain length (hence viscosity) increases. Thus, we believe that the data reported here had sufficient time to become equilibrated. These results for HCl absorption into the acidic IL's derived from different R-groups appear to show a single value for the equilibrium absorption coefficient, $K_{absorption}$, equal to $0.0327 \pm 0.002\ atm^{-1}$. Campbell and Johnson [23] reported HCl solubility data as an equation (#5, p. 7793) for the neutral and acidic IL's. They showed a slightly higher value than our reported value for the absorption coefficient into acidic chloroaluminates derived from the EMIM-Cl IL ($x_{AlCl3} = 2/3$, $K = 0.0337 \pm 0.004\ atm^{-1}$). The values of the absorption coefficients (K) reported by us and others [23] are within experimental error and thus can be considered the same. K-values were also determined for the neutral IL derived from BMIM-Cl ($0.061\ atm^{-1}$), from EMIM-Cl ($0.051\ atm^{-1}$) and a basic IL ($n = 1/2$) also derived from BMIM-Cl ($0.70\ atm^{-1}$). The K-value reported here for the neutral IL derived from EMIM-Cl

was slightly lower than that reported by Campbell and Johnson (0.051 versus 0.062 atm^{-1}) [23]. The *K*-value that we report for the basic melt ($n = 1/2$) cannot be compared to the correlated data reported by Campbell and Johnson. However, our data for $n = 1/2$ fall between curves (a) and (b), Fig. 2A, p. 7794 in Ref. [23]. These two curves reflect the ternary HCl solubility into imidazolium-chloride–HCl (curve a) and $AlCl_3$/ImCl = 0.451 mol/0.549 mol (curve b).

The reported value of the average equilibrium absorption coefficient ($0.0327 \pm 0.002\ atm^{-1}$) corresponds to a free energy of absorption equal to 2 kcal/mol. The AM-1 model predicts a similar value for the free energy of absorption (4.0 kcal/mol) when one considers siting most of the HCl between the cation/anion (structure in Fig. 2b). This model predicts that very little of the HCl would be sited totally on the anion since its free energy of absorption (13 kcal/mol) is so much larger that the free energies for the other two structures. The AM-1 model for structure in Fig. 2c shows HCl having a bond distance similar to that predicted for isolated HCl. These results are consistent with the reports that molecular HCl has been observed in the NMR spectrum of HCl gas in acidic chloroaluminates derived from the $EMIM^+$ cation [20]. In addition, another type of HCl species (structure in Fig. 2b) was predicted by this model which shows an HCl species with a bond length of 1.32–1.36 Å. The $\Delta G_{absorption}$ into the IL predicted by the PM3 model was 0.9–4.3 kcal/mol for all three sites. These predicted $\Delta G_{absorption}$ are similar to the measured value of 2 kcal/mol. The MNDO model also predicted $\Delta G_{absorption}$ that were close to the observed value (2.5–2.6 kcal/mol) when it is considered that few HCl molecules will be sorbed into the higher energy sites (16.9 kcal/mol). Thus, all three, semi-empirical methods predicted $\Delta G_{absorption}$ for HCl into the IL's that were remarkably similar to the observed value of 2.0 kcal/mol.

The gas mixtures experiment showed that CO absorption was not enhanced by the presence of HCl, within the detection limits of the apparatus. We speculate that either we were not able to detect any CO solubility even after the HCl addition, or that the CO was displacing the HCl absorbed while reaching equilibrium, and in this case we were not able to detect any pressure difference. A more powerful tool such as NMR could be used to measure the solubility of ^{13}CO in the IL [12].

The toluene carbonylation reaction has been modeled by an electrophilic substitution mechanism whereby dissolved CO is protonated to form the formyl cation $(HCO)^+$ which then attacks the arene to produce the aldehyde and regenerate the proton [26]. This mechanism is generally accepted as the way to explain most of the data observed for this carbonylation. An alternative mechanism, the intracomplex reaction, suggests that the formation of the electrophile HCO^+ occurs within the complex of proelectrophile and protonated aromatic compounds [27], Eqs. (3) and (4):

$$ArH + H^+ \leftrightarrows ArH_2{}^+ \tag{3}$$

$$ArH_2{}^+ + CO \rightarrow \underset{\pi\text{-complex}}{[ArH_2{}^+CO]} \rightleftarrows \underset{\pi\text{-complex}}{[ArHC(H)O^+]} \rightarrow \underset{\sigma\text{-complex}}{[ArHC(H)O]} \rightarrow ArCOH + H^+ \tag{4}$$

The mechanisms differ by the way they orchestrate the regioselectivity of the reaction. In the case of the intracomplex reaction, the regioselectivity can be heavily influenced by the stability of the protonated arene isomer. The logical extension of this concept is that certain regioisomers of the products are selectively excluded from the product slate when the free energy of the corresponding protonated arene isomer is much higher than the free energies of the other, protonated arene isomers.

Both mechanisms require super acidic protons to produce the required intermediates. In this connection, dissolved HCl is not sufficiently acidic to initiate the reaction as made evident in the control reaction having no IL present. Thus, the introduction of IL into the system develops a super acidic species. While our work does not conclusively identify this super acidic species, the modeling and the experimental work does lead us to speculate that some type of activated HCl is necessary to initiate the reaction. Moreover, this species is generated only when the IL is intrinsically acidic ($n > 1$) regardless of the amount of HCl dissolved into the IL.

We can only speculate on the reactivity of species in the IL towards the toluene carbonylation reaction, but it has been shown that: (1) HCl does absorb into toluene in significant amounts (~0.05 mol/mol toluene at 1.2 atm) at room temperature, (2) molecular modeling shows that HCl associates with the substrate, but that the H–Cl bond distance is only slightly longer than isolated HCl in the gas phase, and (3) that toluene, HCl, and CO in the absence of IL does not react at room temperature. Moreover, when the IL's were made more basic by decreasing the $AlCl_3$/RMIM-Cl ratio from 2 to 1/2, it was observed that the total HCl absorption increased. However, the neutral and basic IL's were unreactive [6,7] towards the toluene carbonylation reaction and thus the increased amount of HCl absorption in these neutral and basic IL's did not contribute to their reactivity. Accordingly, we suggest that more than one type of HCl species is present in the IL's and some of these HCl species may be unreactive towards the toluene carbonylation reaction. We conjecture that structures predicted to have the longer H–Cl bond lengths in IL's (Fig. 2a: 1.53 Å and b: 1.32–1.35 Å) may be the reactive species having some activity for toluene carbonylation but additional experimentation will be necessary to confirm this speculation.

The data of toluene carbonylation show reaction rate constants that decrease from 4.7 to $1.4 \times 10^{-3}\ min^{-1}$ with increasing length of the R-group in the imidazolium cation, and these data, free from mass transport effects, do not appear to correlate with the total HCl absorption into the same IL's. A significant amount of the total HCl absorption into the IL with toluene present (~0.05 mol HCl/mol toluene) appears in

the toluene itself, while an equal amount appears in the IL. In addition, the CO absorption was apparently below the detection limit for our volumetric apparatus. Indeed, the detection limit of the instrument used here corresponds to a CO absorption that was greater than what was observed by Ohlin et al. [12] for CO absorption into a non-acidic IL having the same cations as was examined here. Toluene was miscible in the IL's when HCl was added to the gas phase, which suggests that toluene solubility in the IL is not a limiting factor. These results indicate that the variation in the reactivity with increasing chain length of the R-group cannot be correlated to the total amount of HCl absorption or toluene solubility. The apparatus here was not sufficiently sensitive to detect CO absorption.

Modeling of the same liquids for HCl absorption suggests that more than one type of HCl absorbed species is present, and the reactive species, a Brønsted acid derived from absorbed HCl, could be present in amounts much different that what observed for the total HCl pickup. Therefore, additional experiments will be needed: (1) to determine if multiple HCl species are present in the acidic melts and characterize them for acidity, and (2) to quantitate the CO uptake as was done by Ohlin et al. [12].

5. Summary

The length of the R-group in a family of organic cations apparently plays an important role in the chemistry of toluene carbonylation reaction. The activity for the toluene carbonylation reaction demonstrated a systematic decrease as the chain length in the cation was increased. Modeling of the IL by semi-empirical methods showed that three types of structures were predicted for the HCl/IL and that the free energy of formation for these three structures was different. The predicted free energy of HCl absorption into the IL's was remarkably close to the observed free energy of absorption when one considers the absorption of HCl as structures Fig. 2b and c. Moreover, the H–Cl bond lengths were predicted to be different for the HCl in the different structures. In this work we showed that the variation in the reactivity as R was changed could not be correlated to the amount of HCl absorbed in the ionic liquid since all of the IL's showed similar absorption amounts for HCl. The amount of CO dissolved in the IL's was apparently below the detection limit of the apparatus used here.

Acknowledgments

We gratefully acknowledge the support from Advanced Materials WI Technologies Inc. (Woodstock, GA), the U.S. Department of Education for a GAANN Award to E.A., and from the Georgia Institute of Technology Molecular Design Institute, under prime contract N00014-95-1-1116 from the Office of Naval Research.

References

[1] P. Smith, A.S. Dworkin, R.M. Pagni, S.P. Zingg, Brønsted super acidity of HCl in liquid chloroaluminate, $AlCl_3$-1-ethyl-3-methyl-1*H*-imidazolium chloride, J. Am. Chem. Soc. 111 (1989) 525.
[2] R.Y. Saleh, Process for making aromatic aldehydes using ionic liquids, WO-00/15594, US-6,320,083 (2000).
[3] K. Qiao, Y. Deng, Alkylations of benzene in room temperature ionic liquids modified with HCl, J. Mol. Catal. A: Chem. 171 (2001) 81–84.
[4] S.J. Nara, J.R. Harjani, M.M. Salunkhe, Friedel–Crafts sulfonylation in 1-butyl-3-methylimidazolium chloroaluminate ionic liquids, J. Org. Chem. 66 (2001) 8616–8620.
[5] J.A. Boon, J.A. Levisky, J.L. Pflug, J.S. Wilkes, Friedel–Crafts reactions in ambient-temperature molten salts, J. Org. Chem. 51 (1986) 480–483.
[6] E.J. Angueira, M.G. White, Arene carbonylation in acidic, chloroaluminate ionic liquids, in: Proceedings of the AIChE Annual meeting, San Francisco, CA, November, 2003 (paper 511a).
[7] E.J. Angueira, M.G. White, Arene carbonylation in acidic, chloroaluminate ionic liquids, J. Mol. Catal. A 227/1–2 (2005) 51–58.
[8] C.L. Hussey, H.A. Oye, Transport numbers in molten acidic aluminum chloride—1-methyl-3-ethyl imidazolium chloride. Their relationship to emf measurements in chloroaluminate melts, J. Electrochem. Soc. 131 (1984) 1621.
[9] A.A. Fannin Jr., D.A. Floreani, L.A. King, J.S. Landers, B.J. Piersma, D.J. Stech, R.L. Vaughn, J.S. Wilkes, J.L. Williams, Properties of 1,3-dialkylimldazollum chloride-aluminum chloride ionic liquids. 2. Phase transitions, densities, electrical conductivities, and viscosities, J. Phys. Chem. 88 (1984) 2614–2621.
[10] P. Wasserscheid, W. Keim, Ionic liquids—new solutions for transition metal catalysis, Angew. Chem. 39 (2000) 3772–3789 (Int. ed.).
[11] H. Waffenschmidt, Ph.D. thesis, RWTH, Aachen, Germany (2000).
[12] C.A. Ohlin, P.J. Dyson, G. Laurenczy, Carbon monoxide solubility in ionic liquids: determination, prediction and relevance to hydroformylation, Chem. Commun. (2004) 1070–1071.
[13] F.A. Carey, R.J. Sundberg, Advanced Organic Chemistry. Part a. Structure and Mechanisms, 4th ed., Kluwer Academic/Plenum Publishers, 2000, pp. 46–64.
[14] C.A. Coulson, H.C. Longuet-Higgins, The electronic structure of conjugated systems. II. Unsaturated hydrocarbons and their heteroderivatives, Proc. R. Soc. Ser. A 192 (1947) 16–32;
L. Salem, Intermolecular orbital theory of the interaction between conjugated systems. I. General theory, J. Am. Chem. Soc. 90 (1968) 543–552;
M.J.S. Dewar, R.C. Doughherty, The PMO Theory of Organic Chemistry, Plenum Press, NY, 1975;
G. Klopman, Chemical Reactivity and Reaction Path, Wiley-Interscience, NY, 1974 (Chapter 4).
[15] K. Fukui, Recognition of stereochemical paths by orbital interaction, Acc. Chem. Res. 4 (1971) 57–64;
I. Fleming, Frontier Orbitals and Organic Chemical Reactions, Wiley, NY, 1976;
L. Salem, Electrons in Chemical Reactions: First Principles, Wiley, NY, 1982 (Chapter 4).
[16] K.M. Dieter, C.J. Dymek, N.E. Heimer, J.W. Rovang, J.S. Wilkes, Ionic structure and interactions in 1-methyl-3-ethylimidazolium chloride–$AlCl_3$ molten salts, J. Am. Chem. Soc. 110 (1988) 2722–2726.
[17] W.D. Chandler, K.E. Johnson, Thermodynamic calculations for reactions involving hydrogen halide polymers, ions, and lewis acid adducts. 3. Systems constituted from Al^{3+}, H^+ and Cl^-, Inorg. Chem. 38 (1999) 2050–2056.
[18] E.J. Angueira, M.G. White, Predicting the composition of acidic, ionic liquids in contact with HCl gas, AIChE J., in press.

[19] D.S. Sood, S.C. Sherman, A.V. Iretskii, J.C. Kenvin, D.A. Schiraldi, M.G. White, Formylation of toluene in triflic acid, J. Catal. 199 (2001) 149.
[20] T.A. Zawodzinski, R.T. Carlin, R.A. Osteryoung, Removal of protons from ambient-temperature chloroaluminate ionic liquids, Anal. Chem. 59 (1987) 2639.
[21] H.C. Brown, H. Pearsall, The catalytic halides. I. A study of the catalyst couple, aluminum chloride–hydrogen chloride, and the question of the existence of $HAlCl_4$, J. Am. Chem. Soc. 73 (1951) 4681.
[22] MOPAC 2002 Manual: http://www.cachesoftware.com/mopac/Mopac2002manual/node650.html.
[23] J.L. Campbell, K.E. Johnson, The chemistry of protons in ambient-temperature ionic liquids: solubility and electrochemical profiles of HCl in HCl:ImCl:$AlCl_3$ ionic liquids as a function of pressure (295 K), J. Am. Chem. Soc. 117 (1995) 7791–7800.
[24] J.L. Anthony, E.J. Maginn, J.F. Brennecke, Solubilities and thermodynamic properties of gases in the ionic liquid 1-*n*-butyl-3-methylimidazolium hexafluorophosphate, J. Phys. Chem. B 106 (2002) 7315–7320.
[25] L.P. Davis, C.J. Dymek, J.J.P. Stewart, MNDO calculations of ions in chloroaluminate molten salts, J. Am. Chem. Soc. 107 (1985) 5041–5046.
[26] G.A. Olah, K. Laali, O. Farooq, Superacid-catalyzed formylation of aromatics with carbon monoxide, J. Org. Chem. 50 (1985) 1483–1486.
[27] M. Tanaka, M. Fujiwara, Q. Xu, Y. Souma, H. Ando, K. Laali, Evidence for the intracomplex reaction in Gattermann-Koch formylation in superacids: kinetic and regioselectivity studies, J. Am. Chem. Soc. 119 (1997) 5100–5105.